Porous In_2O_3 Nanorods: Synthesis and Enhanced NO_x Gas-Sensing Properties at Room Temperature

Wenyi LIU, Wencheng FANG, Shuai ZHANG, Guizhi LIU, Yue SUN, Cheng WANG, Chengxin ZHANG, Na GAN, Ying YANG

Key Laboratory of Applied Chemistry and Nanotechnology at Changchun University of Science and Technology

Changchun, 130022, P. R. China

e-mail: yangying0807@126.com

***Abstract*—A novel room temperature gas sensor based on porous In_2O_3 nanorods was successfully synthesized via a facile reflux method. The In_2O_3 demonstrates a rod-like shape with a diameter of 10 - 20 nm and a length about 70 - 100 nm, which displays good and uniform size. Studies have shown that the porous In_2O_3 nanorods have the n-type semiconductor characteristic. We demonstrate that it can detect NO_x gas with a sensitivity of 17, fast response of 17.3 s to 97.0 ppm NO_x and a low detection limit of 0.485 ppm at room temperature.**

Keywords-In_2O_3 nanorods ; NO_x ; gas-sensing

I. Introduction

Design and fabrication of gas sensing devices has been considered to be one of the most important technological developments for public security, biological detection, and monitoring of agriculture, medical, and manufacturing environments. Particularly, NO_x (NO and NO_2) sensors have attracted more attention. Therefore, it is important and necessary to develop reliable NO_x gas sensors to detect very low gas. The NO_x sensors with excellent performance and their composites have been reported in the literature[1 - 3].

In most studies, semiconducting In_2O_3 has widely been studied and applied in catalysts[4], solar water splitting[5] and gas sensors for the detection of NH_3[6], H_2S[7], NO_x[8], ethanol[9], etc. Li et al. have reported that high aspect ratio porous In_2O_3 nanobelts are used at 320 for ethanol detection and 370 for methanol and acetone detection[10]. Gai et al. have studied nitrogen-doped In_2O_3 nanocrystals used as gas sensor towards ethanol at 300 [11]. Xu et al. have investigated In_2O_3 nanorod clusters as gas sensor for NO_2 at 150 [12]. However, those In_2O_3 based gas sensor all operated at relatively high temperature. Therefore, it will be a worthy research topic to synthesize excellent In_2O_3 sensing materials at room temperature.

Herein we demonstrate a facile fabrication of porous In_2O_3 nanorods by reflux method. The porous In_2O_3 nanorods gas sensor possesses an enhanced electrical conductivity, which results in an improved response time towards NO_x at room temperature. The possible response mechanism will be deduced in this paper.

II. Experimental

A. Preparation of In_2O_3 nanorods

All chemicals were of analytical grade and used as received without further purification. Deionized water was homemade. For a typical preparation of the porous In2O3 nanorods, the In(NO3)36H2O (1.2 g) was dispersed in water, giving a dispersion by ultrasonication. By adding a certain amount of urea into the above suspension, which was then reflux distilled for 3 h at 100 under magnetic stirring, the precipitate was obtained. The product was then washed by deionized water several times after cooling to room temperature. Finally, the product was dried at 60 for 10 h in an oven to produce white powder. The obtained material was synthesized by the calcined under an air atmosphere at 550 for 4 h, with a heating rate of 2 min-1.

B. Material Characterizations

The morphologies of the synthesized samples were studied by transmission electron microscopy (TEM, JEOL-JEM-2100, 200 kV). The Brunauer-Emmett-Teller (BET) surface area of the products was measured by using N2 adsorption-desorption (TriStar II 3020); the sample was dried 10 h at 150 under vacuum before the measurement.

C. Gas Sensing Tests

An interdigitated Au electrode (750.38 mm) was selected for gas sensing detection and the electrode spacing was 20 m. A certain amount of sample was dispersed in ethanol to form a suspension, then the suspension was spin-coated onto the interdigitated electrode to form a sensitive film and dried at 70 for 5 h to obtain a thin film gas sensor. The sensor was installed into a test chamber with an inlet and an outlet. The chamber was flushed with air for 2 min to remove any contaminants from the flask and also to stabilize the film before testing. A syringe was used to inject the required volume of NOx vapor into the chamber. The changes in electrical resistance of the sample over time were recorded by a home-made automatic resistance apparatus, and the chamber was purged with air to recover the sensor resistance. The sensor response was defined as the ratio (RN-R0)/R0, where R0 is the sensor resistance in air, and RN is the resistance in NOx gas. The response time is defined as the time required for the variation in resistance to reach 85 % of the equilibrium value after a test gas was injected. The test was conducted at room temperature (20) with a relative humidity (RH) around 40 %.

III. Results and Discussion

A. *Structure and Morphology Characterization of Porous In_2o_3 Nanorods*

The morphologies of the synthesized samples were studied by TEM. Figure 1a shows In2O3 demonstrates a rod-like shape. According to Figure 1b, the porous In2O3 nanorods are composed of nanorod with a diameter of 10 - 20 nm and a length about 70 - 100 nm. It can be easily confirmed that porous In2O3 nanorods are highly crystalline in the TEM image as shown in Figure 1c-d. The measured clear lattice fingers of 0.29 nm and 0.25 nm correspond to the (222) and (400) crystal planes of the porous In2O3 nanorods crystal.

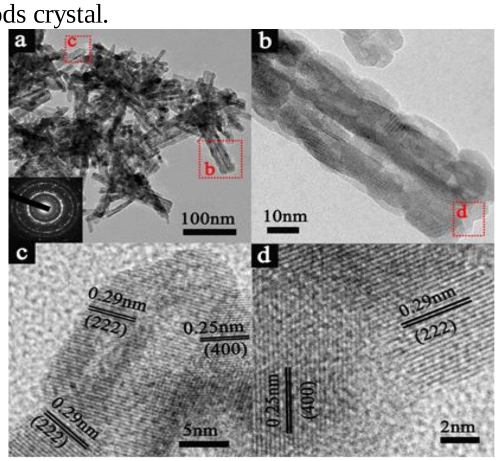

Figure 1. The TEM images of the synthesized In_2O_3

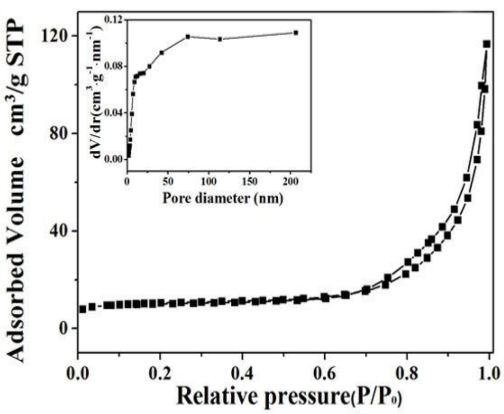

Figure 2. Nitrogen adsorption/desorption isotherm and the corresponding pore size distribution (inset) of the synthesized In_2O_3.

TABLE I. The Results of The Surface Area, Pore Volume and Pore Size.

Sample	S_{BET} (m^2 g^{-1})	pore volume (cm^3 g^{-1})	pore size (nm)
porous In_2O_3 nanorods	36.33	0.16	21.21

In order to further confirm the surface area, pore volume and pore size, the porous In2O3 nanorods were characterized by nitrogen adsorption-desorption measurements to estimate the properties. From the nitrogen adsorption-desorption cyclic curves in Figure 2, the porous In2O3 nanorods sample gives typical type IV isotherms with a clear H3-type hysteresis loop, respectively. It is noticeable that the type of hysteresis clearly resembles the hysteresis observed for layered structure which forms the mesoporous. The BET surface areas, pore volume and pore size of the porous In2O3 nanorods are listed in Table I. The BET surface area of porous In2O3 nanorods is 36.33 m2 g-1, the dominant pore volume and pore size of porous In2O3 nanorods are 0.16 cm3 g-1 and 21.21 nm, respectively. Simultaneously, this results correspond to the TEM images.

B. *Sensing Performance Of Porous In_2o_3 Nanorods*

TABLE II. The Sensitivity and Response Time Results of the Porous In_2O_3 Nanorods Gas Sensor To 97.0 ~ 0.485 ppm NO_x At Room Temperature

NO_x concentration/ ppm	97.0	48.5	29.1	9.70	4.85	0.97	0.485
Sensitivity	17.00	9.99	7.36	5.39	5.06	2.15	1.73
Response time/s	17.3	422.0	470.0	492.6	320.0	130.0	203.3

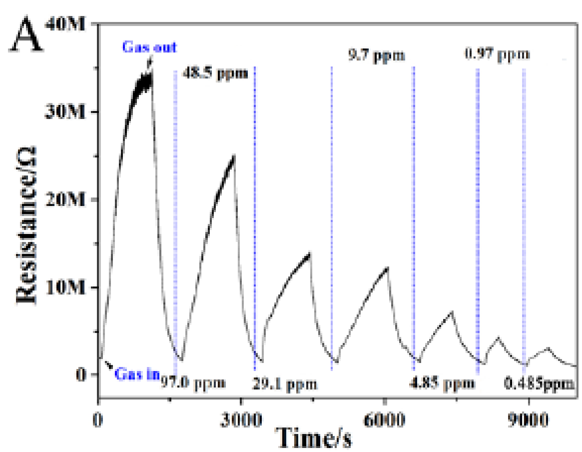

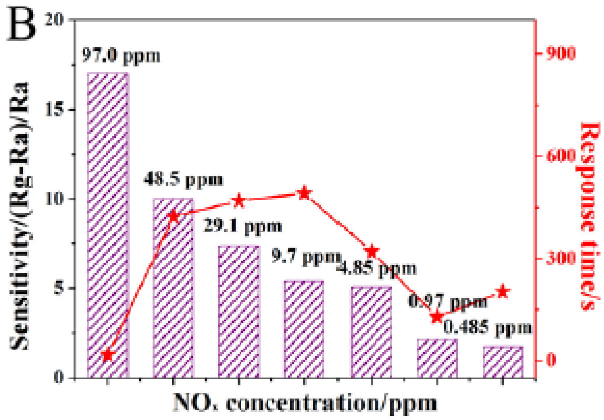

Figure. 3. The results of the gas response of porous In_2O_3 nanorods sensor to 97.0 ppm - 0.485 ppm NO_x operated at room temperature in air. (a) The representative response-recovery cyclic curves; (b) corresponding sensitivity and response time

The gas sensor of the porous In2O3 nanorods is fabricated and investigated at different concentrations of NOx gas. The Figure 3a shows the response and recovery of the gas sensors fabricated from the porous In2O3 nanorods upon exposure to different concentrations of NOx ranging from 97.0 to 0.485 ppm at room temperature in air. It is evident that the gas response amplitude is highly dependent on gas concentration. A sharp increase in surface resistance of the film has been observed with the introduction of NOx and a dramatic drop to its initial value after the sensor was exposed to air. According to the previous literature[13, 14], decrease in the resistance of the gas sensor in oxidizing gas atmosphere shows that the porous In2O3 nanorods are n-type semiconductor. When n-type semiconductor is exposed to NOx gas molecules, the concentration of electron on the surface of the semiconductor decreases due to the loss of an electron as NOx has a higher electron affinity, which results in an increase in resistance of the semiconductor. The corresponding relationship between sensitivity and response time at different NOx concentrations is shown in Figure 3b. When the concentration of NOx is 97.0 ppm, the response time is 17.3 s, while the highest sensitivity can reach 17. And a low detection limit of 0.485 ppm at room temperature. Detailed results of sensitivity and response time are listed in Table II.

C. Sensing Mechanism

When the n-type porous In2O3 nanorods semiconductor is used in gas sensor and exposed in air, O2 molecules will be chemisorbed and capture some electrons of porous In2O3 nanorods to be changed into O2, O, and O2 on the sensing body surfaces. When the sensor film is exposed to NOx, the NOx gas molecules could attract the electrons from the

$$NO_2 + e^- \rightleftarrows NO_2^- \qquad (1)$$

$$NO + e^- \rightleftarrows NO^- \qquad (2)$$

$$NO_2 + O^- \longrightarrow NO_3^-(s) \qquad (3)$$

$$NO + O^- \longrightarrow NO_2^-(s) \qquad (4)$$

porous In2O3 nanorods sensor because of the high electron affinity of the NOx molecules, which leads to electron transfer from the porous In2O3 nanorods. The reactions are as follows:

In a word, when the porous In2O3 nanorods are exposed to air at room temperature, oxygen molecules on the surface capture more electrons from the porous In2O3 nanorods. Effective gas diffusion by the pores on the surface of the porous In2O3 nanorods may contribute to this gas sensing. The pores can act as channels for gas diffusion, and thus provide more active sites for the reaction of NOx with surface-adsorbed oxygen ions. It is beneficial to formation of more chemisorbed oxygen species in the surface, increasing gas sensing property.

IV. Conclusion

In summary, we have synthesized porous In2O3 nanorods and fabricated the material into gas sensor towards NOx gases at room temperature. The porous In2O3 nanorods sensor shows good gas sensing performance, and the lowest testing limit of the sensor is as low as 0.485 ppm NOx for which the sensitivity and response time are 1.73 and 203.3 s, respectively. The porous In2O3 nanorods as a sensing device is potentially superior to other components.

Acknowledgments

We gratefully acknowledge the support of this research by the National Natural Science Foundation of China (No 51572034, 21501104, 201401012, 201501014, 201601018), the Natural Science Foundation of Heilongjiang Province (B2015014), Science and technology project of Jilin Province (20140520079), the Natural Science Foundation of Changchun University of Science and Technology (No. XQNJJ-2015-07, XQNJJ-2013-10).

References

[1] S. Park, S. An, H. Ko, C. Jin, Lee. C, *ACS Appl. Mater. Interfaces* 2012, 4, 3650.

[2] C. Marichy, N. Donato, M. G. Willinger, M. Latino, D. Karpinsky, S. H. Yu, G. Neri, N. Pinna, *Adv. Funct. Mater.*, 2011, **21**, 658.

[3] N. D. Hoa, S. A. El-Safty, *Chem.* Eur. J., 2011, 17, 12896.

[4] L. H. Yu, Y. Huang, G. C. Xiao and D. Z. Li, *J. Mater. Chem. A*, 2013, 1, 9637.

[5] B. Joshi, H. Yoon, H. Kim, M. W. Kim, M. G. Mali, S. S. Al-Deyab and S. S. Yoon, *RSC Adv.*, 2015, 5, 85323.

[6] H. H. Jiang, L. C. Zhao, L. G. Gai, L. Ma, Y. Ma and M. Li, *CrystEngComm*, 2011, 13, 2557.

[7] L. Yin, D. L. Chen, M. X. Hu, H. Y. Shi, D. W. Yang, B. B. Fan, G. Shao, R. Zhang and G. S. Shao, *J. Mater. Chem. A*, 2014, **2**, 18867.

[8] J. Gao, L. L. Wang, K. Kan, S. Xu, L. Q. Jing, S. Q. Liu, P. K. Shen, L. Li and K. Y. Shi, *J. Mater. Chem. A*, 2014, 2, 949.

[9] S. J. Kim, I. S. Hwang, C. W. Na, I. D. Kim, Y. C. Kang and J. H. Lee, *J. Mater. Chem.*, 2011, 21, 18560.

[10] Y. S. Li, J. Xu, J. F. Chao, D. Chen, S. X. Ouyang, J. H. Ye and G. Z. Shen, *J. Mater. Chem.*, 2011, 21, 12852

[11] L. G. Gai, L. Ma, H. H. Jiang, Y. Ma, Y. Tian and H. Liu, *CrystEngComm*, 2012, 14, 7479.

[12] X. M. Xu, H. J. Zhang, C. Z. He, C. Y. Pu, Y. M. Leng, G. Q. Li, S. J. Hou, Y. S. Zhu, L. Fu and G. Y. Lu, *RSC Adv.*, 2016, 6, 47083.

[13] K. I. Choi, S. J. Hwang, Z. F. Dai, Y. C. Kang and J. H. Lee, *RSC Adv.*, 2014, 4, 53130.

[14] K. Grossmann, R. G. Pavelko, N. Barsan and U. Weimar, *Sens. Actuators. B*, 2012, 166, 787.